 DOI: 10.1111/j.1539-6924.2011.01600.x

Influenza Infection Risk and Predominate Exposure Route: Uncertainty Analysis

Rachael M. Jones[1,*] and Elodie Adida[2]

An effective nonpharmaceutical intervention for influenza interrupts an exposure route that contributes significantly to infection risk. Herein, we use uncertainty analysis (point-interval method) and Monte Carlo simulation to explore the magnitude of infection risk and predominant route of exposure. We utilized a previously published mathematical model of a susceptible person attending a bed-ridden infectious person. Infection risk is sensitive to the magnitude of virus emission and contact rates. The contribution of droplet spray exposure to infection risk increases with cough frequency, and decreases with virus concentration in cough particles. We consider two infectivity scenarios: greater infectivity of virus deposited in the upper respiratory tract than virus inhaled in respirable aerosols, based on human studies; and equal infectivity in the two locations, based on studies in guinea pigs. Given that virus have equal probability of infection throughout the respiratory tract, the mean overall infection risk is 9.8×10^{-2} (95th percentile 0.78). However, when virus in the upper respiratory tract is less infectious than inhaled virus, the overall infection risk is several orders of magnitude lower. In this event, inhalation is a significant exposure route. Contact transmission is important in both infectivity scenarios. The presence of virus in only respirable particles increases the mean overall infection risk by 1–3 orders of magnitude, with inhalation contributing $\geq$99% of the infection risk. The analysis indicates that reduction of uncertainties in the concentration of virus in expiratory particles of different sizes, expiratory event frequency, and infectivity at different sites in the respiratory tract will clarify the predominate exposure routes for influenza.

KEY WORDS: Exposure route; infection risk; influenza; uncertainty analysis

1. INTRODUCTION

Though influenza pandemics remain significant threats to the public's health,[1,2] uncertainty persists over the predominate route of influenza transmission: (1) contact, (2) inhalation, (3) inspiration, or (4) direct spray. This information is less important to pandemic control when vaccines and antiviral medications are available, but the experience with 2009 H1N1 suggests that these pharmaceutical interventions may be delayed, inadequate, or ineffective.[3–5] In this context, nonpharmaceutical interventions—for example, frequent hand washing, surface disinfection, the use of respiratory protection, and increased social distancing—are important ways of controlling the pandemic.[1] The selection of effective nonpharmaceutical interventions requires, however, understanding the contribution of each transmission route to infection risk.

Contact transmission involves the deposition of virus onto the eyes, nostrils, and/or lips from the

[1]School of Public Health, University of Illinois at Chicago.
[2]Department of Mechanical and Industrial Engineering, University of Illinois at Chicago.
[*]Address correspondence to Rachael M. Jones, School of Public Health, University of Illinois at Chicago, 2121 W Taylor St, Chicago, IL 60612, USA; tel: 312-996-1960; fax: 312-996-6904; rjones25@uic.edu.

contact of virus-contaminated surfaces (e.g. fingertips), and subsequent transport of virus to tissues with the appropriate influenza receptors.[6,7] Inhalation transmission involves the inhalation of influenza virus in respirable particles (aerodynamic diameters, $d_a \leq 10$ μm), which deposit throughout the upper and lower respiratory tract. Inspiration transmission involves the inspiration of particles ($10 < d_a \leq 100$ μm), which deposit in the upper respiratory tract. Inhalation and inspiration are distinguished because the likelihood of infection in the lower and upper respiratory tract may differ due to the localization of receptors and temperature gradients.[8–13] Direct spray transmission involves the projection of virus carried in cough and sneeze particles (generally $d_a > 100$ μm) onto the eyes, nostrils, and lips.

Experimental influenza research has focused on the effectiveness of nonpharmaceutical interventions,[14–17] rather than the mechanics and magnitude of exposure by each route. In theory, the testing of interventions provides direct information about intervention effectiveness and the predominant exposure route. However, inference from these studies are limited by noncompliance of participants with the interventions, use of multiple interventions, crowding, study design, and specificity of study environments.[18] We suggest that a more generalizable approach is to couple mathematical modeling and experimentation to determine the mechanics of exposure and route-specific infectivity. In this approach, the effectiveness of nonpharmaceutical interventions can be estimated for many environmental contexts, with consideration of the unique transmission aspects of novel influenza viruses.

Furthering this idea, we present an uncertainty analysis of an influenza transmission model previously developed by Nicas and colleagues[12,19] for the context of a susceptible person attending a bedridden infector. We incorporate the analysis of uncertainty in model parameter values by Jones[20] to extend the analysis presented by Nicas and Jones.[12] Our objectives are to: (1) characterize the magnitude and uncertainty of infection risk in this context, (2) quantify uncertainty in predominate transmission route, and (3) identify parameters that determine the predominate transmission route.

2. METHODS

2.1. Exposure Model

The exposure model has been described in detail elsewhere.[12,19] Briefly, a Markov chain describes the movement of virus between select physical elements (states) in a residential bedroom with a bed-ridden infector to estimate the exposure of the attender through contact and the inhalation of respirable virus-laden particles. Exposure via droplet spray and inspiration are modeled separately, as episodic events, due to the low frequency of close-contact during an emission event. Unlike previous implementations,[12] the number of coughs with potential droplet spray and inspiration events is not fixed, but equals the number of coughs emitted in the contact period.

The different Markov chain states correspond to virus located in (1) room air, (2) textile surfaces near the infector, (3) nontextile surfaces near the infector, (4) the attender's hands, (5) the attender's facial membranes, (6) the attender's lower respiratory tract, (7) virus rendered noninfectious by environmental degradation, and (8) exhaust airflow. Virus exchange between state 1 and states 2 and 3 by particle settling from air and resuspension into air, though we assume in this application that no resuspension occurs. Virus can exchange between state 4 and states 2 and 3 via hand contact with surfaces. Virus transferred to states 5, 6, and 8 cannot leave these states. Virus transfers from states 1–4 to state 7 when infectivity is lost. Transfer from state i to state j is described by a first-order rate constant, λ_{ij} (per minute). The probability of a virus moving from state i to state j during time step $\Delta t = 1 \times 10^{-4}$ minute is computed using λ_{ij} and entered into the (ij) cell of the one-step transition probability matrix $\mathbf{P}$, an 8×8 matrix. After n time steps, the probability that an infective virus initially in state $i = \{1, 2, 3\}$ is in state $j = \{5, 6\}$ is the (i, j) entry of the matrix $\mathbf{P}$ multiplied by itself n times, designated $P_{ij}^{(n)}$.

The expected dose to the facial membranes, denoted $E[D_5]$, and to the lower respiratory tract (e.g., inhaled respirable particles), $E[D_6]$, after n time steps are computed as:

$$E[D_5] = N_1 P_{15}^{(n)} + N_2 P_{25}^{(n)} + N_3 P_{35}^{(n)}, \qquad (1)$$

and

$$E[D_6] = N_1 P_{16}^{(n)} + N_2 P_{26}^{(n)} + N_3 P_{36}^{(n)}, \qquad (2)$$

where N_1, N_2, and N_3 are the initial virus loads in the room air and on textile and nontextile surfaces near the infector, respectively. The initial virus loads are equated with the steady-state virus loads. N_1 is largely due to virus in respirable particles, while N_2 and N_3 are largely due to virus in inspirable and

larger particles emitted during coughs, which deposit rapidly onto surfaces near the emission point.[21]

We assume that emission of virus by coughs occurs at interval τ (minute), where τ is the inverse of the cough frequency, with the first emission occurring at time $t = \frac{1}{2}\tau$ minute after the attender enters the room. Thus, given K coughs, a total of $K + 1$ intervals ($K - 1$ intervals of length τ minute and 2 intervals of length $\frac{1}{2}\tau$ minute) are modeled. The total dose during the exposure period is computed as follows. At the time of room entry, $t = 0$ minute, the theoretical steady-state values of N_i were assumed, and the model simulated for duration $\frac{1}{2}\tau$ ($n = \frac{\tau}{2\Delta t}$) to compute $E[D_5]_1$ and $E[D_6]_1$, as in Equations (1) and (2). At time $t = \frac{1}{2}\tau$ minute, the N_i are equated with the virus remaining in each state $i = \{1, 2, 3, 4\}$ plus the virus emitted into each state by the first cough. Based on the size distribution of cough particles and uniform virus concentration, few viruses are emitted in respirable particles.[22] Therefore, 1×10^{-4}%, 90%, and 10% of emitted virus are apportioned to states 1, 2, and 3, respectively. The model is then simulated for duration τ ($n = \frac{\tau}{\Delta t}$), and $E[D_5]_2$ and $E[D_6]_2$ computed. This procedure is repeated for each cough plus the interval between the last cough and the end of the exposure period. The total dose is equated with the sum of doses resulting from each interval. For example, the total dose of the facial membranes is computed for K coughs ($K + 1$ intervals) emitted during the exposure period:

$$E[D_5]_{\text{total}} = \sum_{k=1}^{K+1} E[D_5]_k, \tag{3}$$

where k indexes the intervals between coughs.

Infection risk is computed separately for each exposure pathway, under the assumption that a single influenza virus can infect the host with probability α:

$$R = 1 - \exp(-\alpha f E[D]), \tag{4}$$

where $E[D]$ is the expected dose to the target tissue.[23] The value of f, the fraction of dose that moves from the target tissue (deposition site) to susceptible tissues (infection site), is included to account for the context of dose-response studies. For example, Alford[25] inoculated influenza A directly onto naso- and oropharynx tissues, though in naturally occurring infection, only some fraction, f, of inspired or sprayed virus would move from the facial membranes to these target tissues. Values for α have been previously estimated by Nicas and Jones[12] for human aerosol inhalation,[24] human upper-respiratory tract inoculation,[25] and guinea pig upper-respiratory tract inoculation.[26]

The expected dose due to droplet spray and the inhalation of inspirable particles is computed by assuming the attender faces the infector at distance 0.6 m during a cough, and that particles with aerodynamic diameters $d_a > 10$ μm are emitted and spread as a 3-dimensional cone with a 60° angle, as measured in the plane.[19] At this distance, if a cough particle is randomly located in the 0.38 m^2 circle, the probability that it strikes the 15 cm^2 membrane target is 3.9×10^{-3}. The conditional risk of infection from a droplet spray event, $R_{1,\text{spray}}$, is computed as in Equation (4), where the expected dose, $E[D]$, is the product of the probability that one or more particles carrying different numbers of virus hit the target membrane and the number of virus in each particle.[19] Denoting p_c the probability that the attender is in close contact at the time the infector coughs during each of K coughs, the infection risk is:

$$R_{\text{spray}} = 1 - [1 - p_c \times R_{1,\text{spray}}]^K. \tag{5}$$

The inhaled dose of inspirable particles ($10 < d_a < 100$ μm), $D_{1,\text{inspirable}}$, is computed based on the presence of 0.36% of virus emitted in a cough in inspirable particles,[22] and inhalation of 50% of inspirable particles in one breath.[19] If the attender takes one breath after the cough, the infection risk from one cough, $R_{1,\text{inspirable}}$, is computed using Equation (4), with $E[D] = D_{1,\text{inspirable}}$. Infection risk is computed as with droplet spray (Equation (5)).

Overall infection risk is computed using an inclusion-exclusion formula.[19] The model output is the overall infection risk, and the percent of infection risk contributed by each of the four exposure routes, where the percent infection risk equals the infection risk for each exposure route divided by the sum of the infection risks from all exposure routes.

2.2. Parameter Values

Exposure model parameterization is based on Jones.[20] We use the nonparametric median cumulative distribution estimated by 2-stage Monte Carlo simulation, or 1-stage Monte Carlo simulation (inactivation in air, only), or the specified distribution and/or data when data were insufficient for Monte Carlo simulation (Table I).

Distributions describing inactivation rates in air, on textiles (porous substrates), and nontextiles (nonporous substrates) are based on data at all levels of relative humidity.[20,27,28] The inactivation rate

Table I. Parameter Distributions

Variables		Distribution	Percentile		
			10th	50th	90th
Emission variables	Virus concentration[20,30,31] ($\log_{10}$TCID$_{50}$/mL)	Nonparametric CDF	1.32	3.21	4.98
	Cough fluid volume[22,35] (mL)	Uniform [4.0×10^{-4}, 4.4×10^{-2}]	4.8×10^{-3}	2.2×10^{-2}	4.0×10^{-2}
	Cough frequency[20,32–34] (h^{-1})	Nonparametric CDF	5.84	38.5	215
Inactivation rate (min)	Air[20,27,28]	Nonparametric CDF	9.5×10^{-4}	7.5×10^{-3}	9.5×10^{-2}
	Textiles (Porous substrates)[20,29,37]	Nonparametric CDF	2.53×10^{-3}	7.17×10^{-3}	1.80×10^{-2}
	Nontextile (Nonporous substrates)[20,29]	Nonparametric CDF	7.33×10^{-4}	2.20×10^{-3}	4.70×10^{-3}
	Skin[29]	N($\mu = 1.20, \sigma = 0.390$)	0.698	1.20	1.70
Transfer efficiency (proportion)	Skin-to-textiles[29]	LN(GM = 0.0025, GSD = 1.4)	1.62×10^{-3}	2.50×10^{-3}	3.85×10^{-3}
	Skin-to-nontextiles[29]	LN(GM = 0.079, GSD = 1.4)	5.13×10^{-2}	7.90×10^{-2}	1.22×10^{-1}
	Skin-to-skin[29]	LN(GM = 0.046, GSD = 1.4)	2.98×10^{-2}	4.58×10^{-2}	7.05×10^{-2}
Contact rates (touch/min)	Hand-to-face[36]	Weibull(1.28, 1.95)	0.336	1.46	3.73
	Hand-to-textile[12]	LN (GM = 1.0, GSD = 1.4)	0.650	1.00	1.54
	Hand-to-nontextile[12]	LN (GM = 0.50, GSD = 1.4)	0.325	0.50	0.770
Dose parameters	Translocation f_{URT}	Uniform [0.001, 0.10]	0.011	0.051	0.090
	Close contact probability (p_c)	Uniform [0.01, 0.10]	0.019	0.055	0.091

on skin was based on two measurements by Bean *et al.*,[29] to which a normal (N) distribution was fit.

The efficiency of transfer of virus between surfaces upon contact is based on experimental data obtained by Bean *et al.*[29] We represent the transfer efficiency by a lognormal (LN) distribution, with geometric mean (GD) equal to the measured value and we assume geometric standard deviation (GSD) equal to 1.4. Because we use a LN distribution, the transfer efficiency is guaranteed to take positive values. Transfer efficiencies were assumed to be reciprocal, such that the efficiency of transfer from surface 1 to surface 2 equals the efficiency of transfer from surface 2 to surface 1.

Virus emission is modeled mechanistically, using the volume of respiratory secretions emitted in a cough, the concentration of virus in the expiratory fluids, and the frequency of cough. The latter two parameters are as characterized by Jones[20] using clinical data by Treanor *et al.*[30] and Lee *et al.*[31] The frequency of cough is based on observed rates in patients with acute respiratory infection and pneumonia, as no data are available for influenza patients.[20,32–34] Nicas *et al.*[22] estimated 0.044 mL of fluid to be emitted during a cough, while Jones[20] estimated a total emission volume of 4.0×10^{-4} during cough, based on particle size and number distributions measured by Chao *et al.*[35] We represent the emission volume as a uniform distribution over the range $[4.0 \times 10^{-4}, 4.4 \times 10^{-2}]$.

The rate of hand-to-face contact is based on the observations by Nicas and Best,[36] represented by the most likely Weibull distribution (Table I). Data are not available for rates of hand contacts with environmental surfaces. We assumed these rates were lognormally distributed with GSD = 1.4, and GM equal to the rates assumed by Nicas and Jones.[12]

Separate dose-response parameters are used for the inhalation route, for which infection may occur throughout respiratory tract (α_{Inhale}); and contact, inspiration, and spray routes, for which deposited virus is transported to the upper respiratory tract (α_{URT}). Analysis of human infectivity data has indicated $\alpha_{\mathrm{Inhale}} = 0.18$ and $\alpha_{\mathrm{URT}} = 5.7 \times 10^{-5}$ for doses reported as TCID$_{50}$.[12,25,24] Nasal instillation of influenza A/Panama/2007/99 (H3N2) in guinea pigs suggests $\alpha_{\mathrm{URT}} = 0.16$.[12,26] We consider two infectivity scenarios: (1) equal infectivity, $\alpha_{\mathrm{Inhale}} = \alpha_{\mathrm{URT}} = 0.18$, and (2) unequal infectivity, $\alpha_{\mathrm{Inhale}} = 0.18$, $\alpha_{\mathrm{URT}} = 5.7 \times 10^{-5}$.

The fraction of virus deposited on facial mucous membranes that are transported to receptor sites in the upper respiratory tract is unknown. Aerosol inhalation dose-response studies define dose as the virus concentration in inhaled air,[24] which is the unit in this exposure model. We assume $f = f_{\text{Inhale}} = 1$. Intranasal instillation dose-response studies define dose as the virus deposited on the nasopharynx.[25,26] The exposure model, however, estimates the number of virus deposited on the facial mucus membranes. We assume, therefore, that some fraction of virus is transported into the upper respiratory tract: $f = f_{\text{URT}} \sim$ uniform [0.001, 0.1]. The factor f_{URT} is used for contact, inspiration, and spray exposures.

We assume that the probability that the attender is in close contact during a cough, p_c, is uniformly distributed over the range [0.01, 0.1]. There is no observational data regarding the frequency of close contact during coughs, when spray and inspiration exposure may occur. The range has been chosen to reflect that the likelihood of close contact is small.

2.3. Model Simulation

The exposure model was simulated using point estimates for parameter values (i.e., 50th percentile), and Monte Carlo simulation. In each of the B Monte Carlo simulations, a value for each parameter was randomly sampled (probability sampling) and the model simulated. For parameters defined by nonparametric median cumulative distributions,[20] a value was sampled randomly, with replacement. For other parameters, a random value was sampled from the specified probability distribution (Table I). First-order rate constants describing interzone virus transport, and initial loads computed using the 50th percentile parameter values, are presented in Table II.

2.4. Uncertainty Analysis

We used the point-interval method.[38,39] All parameters are equated with their median values. For each parameter of interest, the model is first simulated with the parameter equated with its 10th percentile value, and the model output is denoted p10. Then, the model is simulated with the parameter equated with its 90th percentile value, and the model output is denoted p90. The magnitude and direction of the parameter's influence on the model outcome is summarized in the ratio p90 : p10. If p90 : p10 = 1.0, then the parameter does not influence the model outcome. If p90 : p10 <1.0, then the outcome decreases as the parameter value increases in value across the central 80% range of its probability distribution. If p90 : p10 >1.0, then the outcome increases with increasing parameter values. The relative importance of each parameter is inferred from the magnitudes of p90 : p10.

3. RESULTS

When simulated with all parameters equal to their median values (Tables I and II), and an equal likelihood of infection for virus in the lower and upper respiratory tract ($\alpha_{\text{Inhale}} = \alpha_{\text{URT}} = 0.18$), the overall risk of influenza infection is 1.5×10^{-3}, with the contact, inhalation, inspiration, and spray routes contributing 58%, <1%, <1%, and 41%, respectively.

Table II. Model Inputs for Representative Scenario Using Median Parameter Values

State	Interstate Transfer Rate Constants (per minute)
1	$\lambda_{1,4} = \lambda_{1,5} = 0, \lambda_{1,2} = 4.9 \times 10^{-3}, \lambda_{1,3} = 5.4 \times 10^{-4}, \lambda_{1,6} = 3.1 \times 10^{-4}, \lambda_{1,7} = 7.5 \times 10^{-3}, \lambda_{1,8} = 8.3 \times 10^{-3}$
2	$\lambda_{2,1} = \lambda_{2,3} = \lambda_{2,5} = \lambda_{2,6} = \lambda_{2,8} = 0, \lambda_{2,4} = 2.8 \times 10^{-6}, \lambda_{2,7} = 7.2 \times 10^{-3}$
3	$\lambda_{3,1} = \lambda_{3,2} = \lambda_{3,5} = \lambda_{3,6} = \lambda_{3,8} = 0, \lambda_{3,4} = 4.0 \times 10^{-4}, \lambda_{3,7} = 2.2 \times 10^{-3}$
4	$\lambda_{4,1} = \lambda_{4,4} = \lambda_{4,6} = \lambda_{4,8} = 0, \lambda_{4,2} = 2.5 \times 10^{-3}, \lambda_{4,3} = 4.0 \times 10^{-2}, \lambda_{4,5} = 1.3 \times 10^{-2}, \lambda_{4,7} = 1.2$
5	$\lambda_{5,1} = \lambda_{5,2} = \lambda_{5,3} = \lambda_{5,4} = \lambda_{5,6} = \lambda_{5,7} = \lambda_{5,8} = 0$
6	$\lambda_{6,1} = \lambda_{6,2} = \lambda_{6,3} = \lambda_{6,4} = \lambda_{6,5} = \lambda_{6,7} = \lambda_{6,8} = 0$
7	$\lambda_{7,1} = \lambda_{7,2} = \lambda_{7,3} = \lambda_{7,4} = \lambda_{7,5} = \lambda_{7,6} = \lambda_{7,8} = 0$
8	$\lambda_{8,1} = \lambda_{8,2} = \lambda_{8,3} = \lambda_{8,4} = \lambda_{8,5} = \lambda_{8,6} = \lambda_{8,7} = 0$
	Initial Virus Load ($TCID_{50}$)
1	$N_1 = 4.7 \times 10^{-5} \times E = 1.7 \times 10^{-3}$
2	$N_2 = 125 \times E = 4500$
3	$N_3 = 45 \times E = 1600$
4	$N_4 = 0 \times E = 0$

Table III. Point-Interval p90 : p10 Ratio Uncertainty Analysis Given Equal Infectivity and Unequal Infectivity

		p90 : p10 Ratio									
		Equal Infectivity					Unequal Infectivity				
		Overall	Percent Risk Contributed by				Overall	Percent Risk Contributed by			
Variables		Risk	Contact	Inhale	Inspire	Spray	Risk	Contact	Inhale	Inspire	Spray
Emission variables	Virus concentration	3000	1.5	1.5	1.5	0.36	4600	1.0	1.0	1.0	0.97
	Cough fluid volume	8.7	0.96	0.96	0.96	1.1	8.4	0.99	0.99	0.99	1.1
	Cough frequency	8.3	0.24	0.41	6.5	6.5	4.6	0.44	0.74	12	12
Inactivation rates	Air	1.0	1.0	0.12	1.0	1.0	0.29	3.4	0.39	3.4	3.4
	Textile	0.97	0.98	1.0	1.0	1.0	0.99	0.97	1.0	1.0	1.0
	Nontextile	0.32	0.50	3.1	3.1	3.1	0.71	0.23	1.4	1.4	1.4
	Skin	0.62	0.73	1.6	1.6	1.6	0.88	0.52	1.1	1.1	1.1
Transfer efficiency	Skin-to-textiles	1.0	1.0	0.99	0.99	0.99	1.0	1.0	1.0	1.0	1.0
	Skin-to-nontextiles	1.6	1.4	0.61	0.61	0.61	1.1	2.0	0.88	0.88	0.88
	Skin-to-skin	1.6	1.4	0.62	0.62	0.62	1.1	2.1	0.88	0.88	0.88
Contact rates	Hand-to-face	3.4	3.2	0.29	0.29	0.29	1.4	7.8	0.72	0.72	0.72
	Hand-to-textiles	1.0	1.0	0.99	0.99	0.99	1.0	1.0	1.0	1.0	1.0
	Hand-to-nontextiles	1.6	1.4	0.62	0.62	0.62	1.1	2.0	0.88	0.88	0.88
Dose parameters	Translocation f_{URT}	7.8	1.1	0.13	0.13	0.94	1.5	5.3	0.65	0.65	5.4
	Close contact probability	1.7	0.57	0.57	2.7	2.7	1.2	0.86	0.86	4.1	4.1

Given unequal infection likelihood in the lower and upper respiratory tract ($\alpha_{Inhale} = 0.18$, $\alpha_{URT} = 5.7 \times 10^{-5}$), the overall risk of influenza infection is 1.8×10^{-6}, with the contact, inhalation, inspiration, and spray routes contributing 15%, 73%, <1%, and 12%, respectively.

To illustrate interpretation of the p90 : p10 ratios (Table III), consider the parameter virus concentration in expiratory fluid and equal infectivity. For the overall infection risk, p90 : p10 = 3000, indicating that overall infection risk increases with the concentration of virus in cough fluid. For the percent of infection risk contributed by each exposure route, p90 : p10 = 1.5 for the contact, inhalation, and inspiration routes, and p90 : p10 = 0.36 for the spray route, which means that the contact, inhalation, and inspiration routes become increasingly important to infection risk, relative to spray exposure, as the concentration of virus increases. In contrast, when infectivity is unequal, increasing virus concentration in the expiratory fluid does not significantly alter the importance of the four infection routes (p90 : p10 ~1.0).

Increasing values of all parameters except inactivation rates increases infection risk (Table III). The influence of textile-related contact rates and transfer efficiencies in the model is small, due to small textile surface area and relatively low contact rate. Increasing contact rates and transfer efficiencies increases the contribution of contact exposure to infection risk, while increasing inactivation rates on skin, textiles, and nontextiles decreases the contribution of contact exposure. While increased cough frequency increases contribution of spray and inspiration exposures to infection risk, increased virus concentration in cough fluid decreases the contribution of spray exposures. The general pattern in p90 : p10 ratios is similar for both infectivity scenarios, though the magnitude of impact on the change in overall infection risk is smaller (p90 : p10 are closer to 1) due to the lower likelihood of infection through the contact, spray, and inspiration routes.

The risk of infection is approximately two orders of magnitude higher for equal infectivity than unequal infectivity. Monte Carlo simulation with equal infectivity predicts mean (median) 9.8×10^{-2} (4.4×10^{-3}), with 90% central range [8.8×10^{-6}, 0.78]. Monte Carlo simulation with unequal infectivity predicts mean (median) overall infection risks of 3.8×10^{-4} (2.8×10^{-6}), with 90% central range [7.6×10^{-9}, 8.4×10^{-4}]. The contribution of spray and contact exposures are higher for equal than unequal infectivity (Fig. 1). In both cases, the inspiration route rarely contributes very much to the overall infection risk.

4. DISCUSSION

The exposure model predicts that the risk of influenza infection arising from a susceptible person

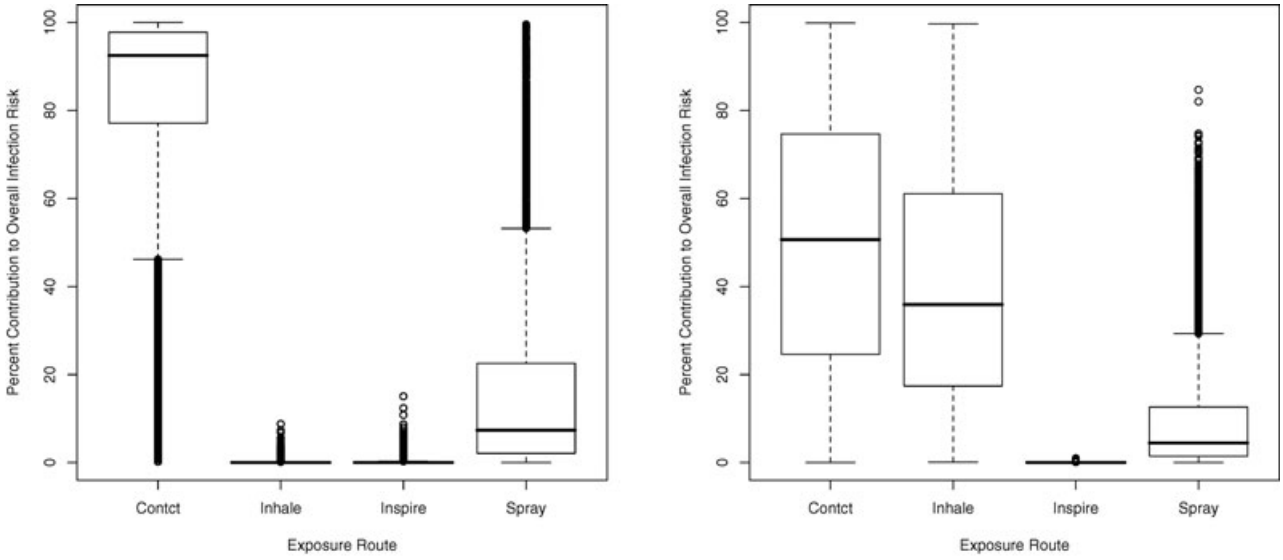

Fig. 1. Contributions of each exposure route to overall infection risk given the equal and unequal infectivity scenarios. The box delineates the 25th, 50th, and 75th percentiles, and the whiskers extend to 1.5 times the interquartile range.

attending a bed-ridden infectious person for 15 minute is relatively low on average, 10^{-2} to 10^{-4}. However, Monte Carlo simulations indicate that some combinations of exposure parameters may yield upper-bound infection risks of 0.78. These risk estimates are in the same range, but not exactly equal to those reported by Nicas and Jones.[12] One difference from those investigators in this work is that the number of potential inspiration and spray exposures equals the number of coughs per exposure period, instead of being fixed at three per exposure period. A limitation of the exposure model is the exclusion of influenza emission in exhaled breath,[40,41] though virus emission through this route is low relative to the emission rates in the exposure model.

We considered two infectivity scenarios based on dose-response studies of influenza virus in humans (unequal infectivity scenario) and in guinea pigs (equal infectivity scenario). In general, infectivity data from human studies are preferred to animal studies, but the studies in humans, particularly of aerosol inhalation,[24] are small and fitted dose-response parameters highly uncertain.[12] As a result, we considered findings in guinea pigs[26] to inform the selection of the infectivity scenarios. When virus is equally likely to initiate infection in the lower and upper respiratory tract, contact and spray exposure routes are more important to infection risk, and the risk of infection is several orders of magnitude higher than when virus is more likely to initiate infection in the lower than upper respiratory tract (Fig. 1). The risk of infection in the upper respiratory tract is influenced by the proportion of virus deposited on the exterior mucous membranes that translocates to susceptible tissues (f_{URT}), particularly in the equal infectivity scenario (p90 : p10 = 7.8). Given the sensitivity of infection risk and exposure route to these infectivity variables (α_{URT}, α_{Inhale}, and f_{URT}), and the localization and specificity of receptors for different influenza viruses,[7–11] it would seem appropriate to explore the infectivity of novel influenza viruses.

Point estimates were used for the dose-response parameters α_{URT} and α_{Inhale} in our analyses, rather than distributions. In the estimation of these parameters from the human infectivity studies of Alford and colleagues,[24,25] Nicas and Jones[12] found α_{URT} and α_{Inhale} to not be statistically significantly different from zero, with 95% confidence intervals $[3.2 \times 10^{-5}, 1.2 \times 10^{-4}]$ and $(0.0, 0.68]$, respectively. Though $\alpha_{\mathrm{URT}} = 5.7 \times 10^{-5}$ and $\alpha_{\mathrm{Inhale}} = 0.18$ are the best-estimates, the lack of statistical significance make it difficult to interpret the probability distribution of these values with confidence. Changing α_{URT} 4 orders of magnitude between the unequal and equal infectivity scenarios (a larger change than anticipated by the 95% confidence interval) increased overall infection risk 2–3 orders of magnitude, and increased

the median contribution of contact transmission from 50% to 95%(Fig. 1). This result indicates that variability in the dose-response parameters is an important determinant in influenza transmission, but given the general insufficiency of available human infectivity data, we judged that the analysis of uncertainty in influenza infection risk from exposure and environmentally related variables to be a more important contribution at this time.

Our uncertainty analysis identified emission variables as strongly influencing the magnitude of infection risk for both infectivity scenarios (Table III). Of the emission variables, only cough frequency alters the relative contributions of the exposure routes (increasing cough frequency increases the contribution of the inspiration and spray routes). The emission of influenza virus from infectious persons, however, remains poorly understood. Though cough is frequently noted amongst influenza patients,[42,43] cough frequency has not been documented. Herein, we used the analysis of Jones,[20] based on observations in persons with acute respiratory illness and pneumonia, where the median cough frequency is 38.5 coughs per hour. The small p90 : p10 ratios for cough frequency and contribution of contact transmission indicates that lower cough frequency is most strongly associated with increased contact transmission. Characterization of expiratory particle size and count distributions has been based on observations of healthy persons.[22,35,44] Persons with influenza may emit more or less volume.

An assumption of the exposure model is that the number of virus per unit volume of expiratory fluid is uniform across the expiratory particles. Studies of *Mycobacterium tuberculosis*[45] and *Pseudomonas aeruginosa*,[46] though limited by the experimental apparatus, suggest that pathogens are more frequently in respirable than larger cough particles. Influenza virus in exhaled breath particles is predominately isolated from particles <0.01 μm in diameter, and these particles are formed by the breaking of fluid films or bubbles during the opening of terminal airways during inhalation.[41,47,48] Cough particles, however, form from wind shear in the respiratory tract, and Morawska[49] has hypothesized that this formation mechanism means that the number of pathogens in an expiratory particle will depend upon where in the respiratory tract the particle was formed, and the site of infection. We explored this idea in our model by assuming that 90% of the emitted virus was in respirable particles. Monte Carlo simulation predicts (for both equal and unequal infectivity) the mean (median) infection risk to be 0.53 (0.52), with the inhalation route contributing $\geq$99% of the infection risk. The value of 90% was chosen to represent an extreme value, but is not inconsistent with the finding that 65% of influenza viral RNA emitted in coughs was in particles with aerodynamic diameters <4 μm.[50] The alteration in magnitude of infection risk and predominant exposure route indicates that further study should be initiated to characterize the distribution of virus in expiratory particles.

Studies of influenza transmission in guinea pigs have found that warm (30 °C), humid conditions (80% RH) reduce transmission via the aerosol route (e.g., inhalation of respirable particles),[51] but do not decrease transmission when susceptible and infectious animals are placed in the same cage (e.g., all possible routes).[52] Though we have not explored the influence of temperature and humidity in particular, our results are consistent with these findings. The uncertainty analysis shows that increasing inactivation rates in air decreases the contribution of inhalation exposure to infection risk (Table III), and laboratory studies of influenza virus aerosols have associated increased temperature and humidity with increased influenza inactivation.[27,28]

Our results provide qualitative insight into the effectiveness of control measures. Given the uniform distribution of virus across expiratory particles by volume, we found spray exposure to contribute significantly to infection risk in the equal infectivity scenario (Fig. 1a). Covering the nose and mouth during coughing and sneezing prevents the projection of virus-laden particles into the environment,[48] while the use of a face shield or respirator by the susceptible person prevents deposition of projected particles. Frequent hand washing, which removes infectious virus from the hands,[53] and reduction in hand-to-face contacts (p90 : p10 $>$1.0, Table III) can interrupt contact exposures. Given the contribution of contact transmission to the overall infection risk (Fig. 1), hand washing and contact reduction may be important interventions. We found that inhalation exposure contributes significantly to infection risk in unequal infectivity scenario (73% given median values; Fig. 1b), and when influenza virus is predominately in respirable particles ($>$99%). Inhalation exposure can only be interrupted by the use of respiratory protection, but respirators simultaneously prevent the spray, inspiration, and contact-related deposition of virus in the mouth and nares.

Modeling studies by Wein and Atkinson[54,55] have found that inhalation of respirable particles is

the predominant route of influenza exposure, and that N95 respirators are the key infection control measure. The infectivity assumptions used by Wein and Atkinson[55] are similar to the unequal infectivity scenario here, but their model utilized a composite parameter reflecting virus transfer that is two-orders of magnitude lower than the equivalent rate estimated by Nicas and Jones,[12] and lower than most values estimated in the Monte Carlo simulations herein. It is, therefore, unsurprising that we find a greater role for contact transmission of influenza. Given current uncertainties in exposure-related variables and infectivity, the predominant route of exposure is uncertain, and the magnitude of infection risk highly variable. Our analysis supports the idea that uncertainties may be reduced by experimental investigation of: the concentration of virus in expiratory particles of different sizes, the frequency of expiratory events, frequency of close expiratory events, and the infectivity of virus strains at different sites of the respiratory tract.

ACKNOWLEDGMENTS

R.M.J. was supported by the Centers for Disease Control and Prevention Training Program Grant 2T01 CD000189-01.

REFERENCES

1. Centers for Disease Control and Prevention. Community Strategy for Pandemic Influenza Mitigation, 2009. Available at: http://www.flu.gov/professional/community/commitigation.html, Accessed on September 15, 2009.
2. Institute of Medicine Committee on Respiratory Protection for Healthcare Workers in the Workplace Against Novel H1N1 Influenza A. Respiratory Protection for Healthcare Workers in the Workplaces Against Novel N1H1 Influenza A. Washington, DC: National Academies Press, 2009.
3. Dimitrov N, Goll S, Meyers LA, Pourbohloul B, Hupert N. Optimizing tactics for use of the U.S. antiviral strategic national stockpile for pandemic (H1N1) influenza, 2009. PLoS Currents: Influenza, 2009; 1:RRN1127.
4. Collin N, de Radigues X, and the World Health Organization H1N1 Vaccine Task Force. Vaccine production capacity for seasonal and pandemic (H1N1) 2009 influenza. Vaccine, 2009; 27:5184–5186.
5. Sullivan SJ, Jacobson RM, Dowdle WR, Poland GA. 2009 H1N1 influenza. Mayo Clinic Proceedings, 2010; 85:64–76.
6. Olofsson S, Kumlin U, Dimock K, Arnberg N. Avian influenza and sialic acid receptors: More than meets the eye? Lancet Infectious Diseases, 2005; 5:184–188.
7. Belser JA, Wadford DA, Xu J, Katz JM, Tumpey TM. Ocular infection of mice with influenza A (H7) viruses: A site of primary replication and spread to the respiratory tract. Journal of Virology, 2009; 83:7075–7084.
8. Shinya K, Ebina M, Yamada S, Ono M, Kasai N, Kawaoka Y. Influenza virus receptors in the human airway: Avian and human flu viruses seem to target different regions of a patient's respiratory tract. Nature, 2006; 440:435–436.
9. van Riel D, Munster VJ, de Wit E, Rimmelzwaan GF, Fouchier RAM, Osterhaus ADME, Kuiken T. H5N1 virus attachment to lower respiratory tract. Science, 2006; 312:399.
10. van Riel D, Munster VJ, de Wit E, Rimmelzwaan FG, Fouchier RAM, Osterhaus ADME, Kuiken T. Human and avian influenza viruses target different cells in the lower respiratory tract of humans and other mammals. American Journal of Pathology, 2007; 171:1215–1223.
11. Scull MA, Gillim-Ross L, Santos C, Roberts KL, Bordonali E, Subbarao K, Barclay WS, Pickles RJ. Avian influenza virus glycoproteins restrict virus replication and spread through human airway epithelium at temperatures of the proximal airways. PLoS Pathogens, 2009; 5:e1000424.
12. Nicas M, Jones RM. The relative contributions of four exposure pathways to influenza infection risk. Risk Analysis, 2009; 29:1292–1303.
13. Mubareka S, Lowen AC, Steel J, Coates AL, García-Sastre A, Palese P. Transmission of influenza virus via aerosols and fomites in the guinea pig model. Journal of Infectious Diseases, 2009; 199:858–865.
14. Aiello AE, Murray GF, Perez V, Coulborn RM, Davis BM, Uddin M, Shay DK, Waterman SH, Monto AS. Mask use, hand hygiene, and seasonal influenza-like illness among young adults: A randomized intervention trial. Journal of Infectious Diseases, 2010; 201:491–498.
15. Larson EL, Ferng Y, Wong-McLoughlin J, Wang S, Haber M, Morse SS. Impact of non-pharmaceutical interventions on URIs and influenza in crowded, urban households. Public Health Reports, 2010; 125:178–191.
16. Loeb M, Dafoe N, Mahony J, John M, Sarabia A, Colavin V, et al. Surgical mask vs N95 respirator for preventing influenza among health care workers: A randomized trial. Journal of American Medical Association, 2009; 302:1865–1871.
17. Cowling BJ, Fung RO, Cheng CK, Fang VJ, Chan KH, Seto WH, et al.. Preliminary findings of a randomized trial of non-pharmaceutical interventions to prevent influenza transmission in households. PLoS One, 2008; 3:e2102.
18. Aiello AE, Coulborn RM, Aragon TJ, Baker MG, Burrus BB, Cowling BJ, et al.. Research findings from nonpharmaceutical intervention studies for pandemic influenza and current gaps in the research. American Journal of Infection Control, 2010; 38:251–258.
19. Nicas M, Sun G. An integrated model of infection risk in a health-care environment. Risk Analysis, 2006; 26:1085–1096.
20. Jones RM. Critical review and uncertainty analysis of factors influencing influenza transmission. Risk Analysis; in press.
21. Hinds WC. Aerosol Technology: Properties, Behavior and Measurement of Airborne Particles, 2nd edition. New York: John Wiley & Sons, Inc., 1999.
22. Nicas M, Nazaroff WW, Hubbard A. Toward understanding the risk of secondary airborne infection: Emission of respirable pathogens. Journal of Occupational and Environmental Hygiene, 2005; 2:143–154.
23. Haas CN, Rose JB, Gerba CP. Quantitative Microbial Risk Assessment. New York: John Wiley & Sons, Inc., 1999.
24. Alford RH. An attempt at protection of man against virulent influenza using nasal instillation of inactivated virus. Annals of Internal Medicine, 1965; 62:1312–1314.
25. Alford RH, Kasel JA, Gerone PJ, Knight V. Human influenza resulting from aerosol inhalation. Proceedings of the Society for Experimental Biology and Medicine, 1966; 122:800–804.
26. Lowen AC, Mubareka S, Tumpey TM, García-Sastre A, Palese P. The guinea pig as a transmission model for human influenza viruses. Proceedings of the National Academy of Sciences USA, 2006; 103:9988–9992.
27. Harper GJ. Airborne micro-organisms: Survival tests with four viruses. Journal of Hygiene (London), 1961; 59:479–486.

28. Hemmes JH, Winkler KC, Kool SM. Virus survival as a seasonal factor in influenza and poliomyelitis. Nature, 1960; 188:430–431.
29. Bean B, Moore BM, Sterner B, Peterson LR, Gerding DN, Balfour Jr HH. Survival of influenza viruses on environmental surfaces. Journal of Infectious Diseases, 1982; 146:47–51.
30. Treanor JJ, Hayden FG, Vrooman PS, Barabarsh R, Bettis R, Riff D, Singh S, Knersley N, Ward P, Mills RG, for the US Oral Neuraminidase Study Group. Efficacy and safety of the oral neuraminidase inhibitor Oseltamivir in treating acute influenza. Journal of the American Medical Association, 2000; 283:1016–1024.
31. Lee N, Chan PKS, Hui DSC, Rainer TH, Wong E, Choi KW, Lui GCY, Wong BCK, Wong RYK, Lam WY, Chu IMT, Lai RWM, Cockram CS, Sung JJY. Viral loads and duration of viral shedding in adult patients hospitalized with influenza. Journal of Infectious Diseases, 2009; 200:492–500.
32. Loudon RG, Brown LC. Cough frequency in patients with respiratory disease. American Review of Respiratory Disease, 1967; 96:1137–1143.
33. Paul IM, Wai K, Jewell SJ, Schaffer ML, Varadan VV. Evaluation of a new self-contained, ambulatory, objective cough monitor. Cough, 2006; 2:7. doi: 10.1186/1745-9774-2-7.
34. Kuhn JJ, Hendley JO, Adams KF, Clark JW, Gwaltney Jr. JM. Antitussive effect of guaifenesin in young adults with natural colds. Objective and subjective assessment. Chest, 1982; 82:713–718.
35. Chao CYH, Wan MP, Morawska L, Johnson GR, Ristovski ZD, Hargreaves M, Mengersen K, Corbett S, Li Y, Xie X, Katoschevki D. Characterization of expiration air jets and droplet size distributions immediately at the mouth opening. Aerosol Science, 2009; 40:122–133.
36. Nicas M, Best D. A study quantifying the hand-to-face contact rate and its potential application to predicting respiratory tract infection. Journal of Occupational and Environmental Hygiene, 2008; 5:347–352.
37. Thomas Y, Vogel G, Wunderli W, Suter P, Witschi M, Koch D, Tapparel C, Kaiser L. Survival of influenza virus on banknotes. Applied and Environmental Microbiology, 2008; 74:3002–3007.
38. Xue J, Zartarian VG, Oezkaynak H, Dang W, Glen G, Smith L, Stallings C. A probabilistic arsenic exposure assessment for children who contact chromated copper arsenate (CCA)-treated playsets and decks, part 2: Sensitivity and uncertainty analyses. Risk Analysis, 2006; 26:533–541.
39. Julian TR, Canales RA, Leckie JO, Boehm AB. A model of exposure to rotavirus from nondietary ingestion iterated by simulated intermittent contacts. Risk Analysis, 2009; 25:617–631.
40. Stelzer-Braid S, Oliver BG, Blazey AJ, Argent E, Newsome TP, Ralwingson WD, Tovey ER. Exhalation of respiratory viruses by breathing, coughing and talking. Journal of Medical Virology, 2009; 81:1674–1679.
41. Fabian P, McDevitt JJ, DeHaan WH, Fung RPO, Cowling BJ, Chan KH, Leung GM, Milton DK. Influenza virus in human exhaled breath: An observational study. PLoS One, 2008; 3:e2691.
42. Cao B, Li XW, Shu Y, Jiang N, Chen S, Xu X, Wang C, and for the National Influenza A Pandemic (H1N1) 2009 Clinical Investigation Group of China. Clinical features of the initial cases of the 2009 pandemic influenza A (H1N1) virus infection in China. New England Journal of Medicine, 2009; 361:2507–2517.
43. Al Kuwaitir TS, Al Abdulkarim AS, Abba AA, Yousef AM, El-Din MA, Rahman KT, Ali MA, Mohamed ME, Arnous NE. H1N1 influenza A: Preliminary evaluation in hospitalized patients in a secondary care facility in Saudi Arabia. Saudi Medical Journal, 2009; 30:1532–1536.
44. Loudon RG, Roberts RM. Droplet expulsion from the respiratory tract. American Review of Respiratory Disease, 196; 95:435–442.
45. Fennelly KP, Martyny JW, Fulton KE, Orme IM, Cave DM, Heifets LB. Cough-generated aerosols of *Mycobacterium tuberculosis*: A new method to study infectiousness. American Journal of Respiratory and Critical Care Medicine, 2004; 169:604–609.
46. Wainwright CE, France MW, O'Rourke P, Anuj S, Kidd TJ, Nissen MD, Sloots TP, Coulter C, Ristovski Z, Hargreaves M, Rose BR, Harbour C, Bell SC, Fennelly KP. Cough-generated aerosols of *Psuedomonas aeruginosa* and other Gram-negative bacteria from patients with cystic fibrosis. Thorax, 2009; 64:926–931.
47. Schwarz K, Biller H, Windt H, Koch W, Hohlfeld JM. Characterization of exhaled particles from the healthy human lung: A systematic analysis in relation to pulmonary function variables. Journal of Aerosol Medicine Pulmonary Drug Delivery, 2010; 23:371–379.
48. Johnson GR, Morawska L. The mechanism of breath aerosol formation. Journal of Aerosol Medicine Pulmonary Drug Delivery, 2009; 22:229–237.
49. Morawska L. Droplet fate in indoor environments, or can we prevent the spread of infection?. Indoor Air, 2006; 16:335–347.
50. Lindsley WG, Blachere FM, Thewlis RE, Vishnu A, Davis KA, Cao G, Palmer JE, Clark KE, Fisher MA, Khakoo R, Beezhold DH. Measurements of airborne influenza virus in aerosol particles from human coughs. PLOSone, 2010; 5:e15100.
51. Lowen AC, Mubareka S, Steel J, Palese P. Influenza virus transmission is dependent upon relative humidity and temperature. PLoS Pathology, 2007; 3:e151.
52. Lowen AC, Steel J, Mubareka S, Palese P. High temperature (30°C) blocks aerosol but not contact transmission of influenza virus. Journal of Virology, 2008; 82:5650–5652.
53. Grayson ML, Melvani S, Druce J, Barr IG, Ballard SA, Johnson PDR, Mastorakos T, Birch C. Efficacy of soap and water and alcohol-based hand-rub preparations against live H1N1 influenza virus on the hands of human volunteers. Clinical Infectious Diseases, 2009; 48:285–291.
54. Wein LM, Atkinson MP. Assessing infection control measures for pandemic influenza. Risk Analysis, 2009; 29:949–962.
55. Atkinson MP, Wein LM. Quantifying the routes of transmission for pandemic influenza. Bulletin of Mathematical Biology, 2008; 70:820–867.